

## PRIMARY STANDARD FOR NANOFLOW RATES

*P. Lucas<sup>1</sup>, H.T. Petter<sup>1</sup>, W. Sparreboom<sup>2</sup>, J.C. Lötters<sup>2</sup>*

<sup>1</sup>Dutch Metrology Institute (VSL), Delft, The Netherlands

<sup>2</sup>Bronkhorst High-Tech, Ruurlo, The Netherlands

Micro- and nanoflows are appearing more frequently in various applications, for example in life science and technology, automotive and lab-on-a-chip applications. Further, they are relevant for some medical applications, for example in (implanted) pain control pumps. For these applications, traceability can be important for a safe and sound usage.

As of yet there does not exist a validated primary standard for flow rates lower than, say, 20  $\mu\text{l}/\text{min}$ . Therefore, this research, which is part of [4], aims at developing a primary standard for liquid volume flows for flow rates from 1 up to 1000  $\text{nl}/\text{min}$ .

The approach followed is a standard based on volumetric expansion (comparable to an old-fashioned thermometer). The upper part of the given flow rate range can also be achieved with a gravimetric principle (e.g. [5]). However, for flow rates lower than, say 100  $\text{nL}/\text{min}$ , the uncertainty due to for example evaporation makes this principle not applicable. Conventional syringe pumps are not feasible because the inner dimensions of the syringe cannot be determined with sufficient low uncertainty. A syringe pump based on a plunger rather than a piston may be an interesting alternative.

Recently, also good results for flow rates between 1 and 1000  $\text{nL}/\text{min}$  have been achieved with a front-tracking system [1]. In this set up the velocity of the meniscus inside a capillary is measured. With the velocity and dimensions of the capillary known, the flow rate is deduced.

In Figure 1 a sketch of the volume-expansion standard is shown; the expanding liquid is contained in a reservoir placed inside a temperature controlled (water) bath. In Figure 2 the reservoir containing the expanding liquid is shown and in Figure 3 the complete set up.

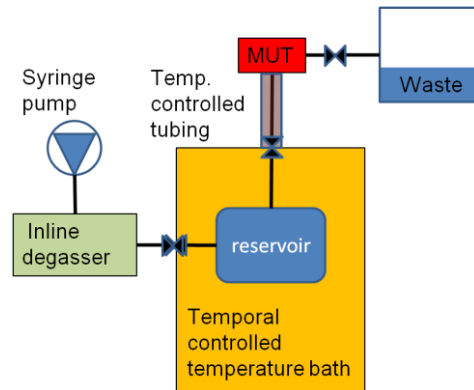


Figure 1. Sketch principle standard.

The driving force is the decrease in density over time. Hence, the flow rate follows from:

$$Q = -\frac{1}{\rho} \frac{dm}{dt}$$

where  $m$  is the mass of the expanding liquid and  $\rho$  is the density at the exit of the reservoir. Working out this equation gives the following main component:

$$Q = -\frac{Vk}{\rho_{MUT}} \left( \frac{\partial \rho}{\partial T} \right)$$

where  $V$  is the volume of the expanding liquid,  $k$  is the temperature gradient,  $\rho$  is the density and  $T$  is the temperature. Since the temperature is time controlled, one has a control over the time rate change of the density and thus also the volume flow rate.

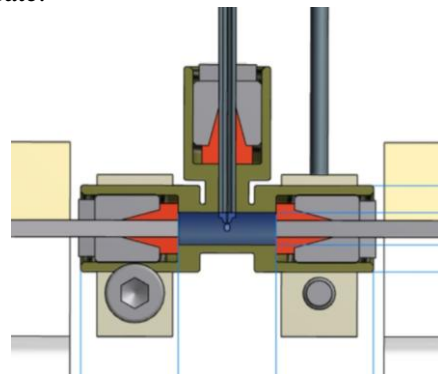
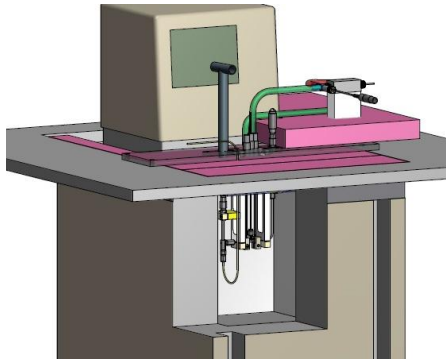


Figure 2 Close up reservoir. The temperature is measured in the center of the reservoir.



*Figure 3 Set up primary standard for nano flow rates. The MUT is shown on the right (in white). The pink material is insulation, whereas the lever shown is to open and close one of the valves.*

Because the flow rate depends on the (temporal) volume, density and liquid properties, the flow rate will be varying for a constant temperature gradient. This is because over time the temperature increases which leads to a different fluid properties. However, for sufficient small temperature gradients, say smaller than 0.02 K/s, the flow rate is fairly constant for at least 10 minutes.

In order to arrive at the correct flow rate, several corrections need to be made to the main component. Corrections are required for: the expansion of the reservoir itself, cooling down of the fluid elements when they travel through the capillaries that are not submerged (see Fig. 3) and a non-homogeneous temperature throughout the whole reservoir. Numerical modeling has been used to estimate the impact of the non-homogeneous temperature distribution [3]. Further, standard equations and material properties have been used to determine the volume expansion of the reservoir. Finally, it is straightforward to show that the impact of the cooling down is negligible when the volume of the capillaries is small compared to the volume of the reservoir, say smaller than 5%.

The flow rate can be made traceable directly to SI units. Therefore one needs to know the following parameters: (temporal) volume of the expanding liquid, temperature gradient and the liquid properties (density and expansion coefficient).

The volume of the expanding liquid follows from the mass difference between an empty and filled reservoir (and correction for the expansion of the reservoir itself). The temperature gradient

follows from temperature measurements inside the reservoir and just outside the reservoir (see Fig. 2). Finally, the liquid properties follow from the Tanaka equation [5]. Hence, pure and degassed water needs to be used.

The estimated uncertainty is around 2.5% ( $k=2$ ), depending on the flow rate. The largest contributions are due to the expansion of the reservoir, the temperature gradient and the spatial variation in the temperature gradient. Linear regression [2] is used to determine the uncertainty in the temperature gradient.

In Fig. 5 a comparison is shown between the volume-expansion, a gravimetric standard and a chip-based Coriolis flow meter [4,5]. This flow meter has been calibrated by a gravimetric standard at zero flow and full scale (2 g/h). The calibration coefficients are then assumed to be constant over the complete range. In Fig. 4 the measured temperature and resulting temperature gradient are shown. From the temperature gradient the flow rate according to the volume-expansion standard is determined.

The top graph of Fig. 5 shows the balance read out. The middle graph shows the unfiltered data as given by the standard and the chip-based Coriolis meter (the results from the gravimetric standard are omitted because they are very noisy). Here, unfiltered means the discrete values are used to determine the temperature gradient. The bottom part of Fig. 5 shows fitted polynomials found by linear regression for a specific part of the calibration. This part is selected because in this part the temperature increase is homogenous throughout the whole reservoir (differences smaller than 1% of the mean temperature gradient). This selection results in a relative low uncertainty because the expansion of the water is only well-known in case the (temporal) temperature gradient is constant throughout the whole reservoir. In case all measurement data is included, the calibration uncertainty easily increases to 5% or more.

For the selected data points, the average deviation between the standard and chip-based flow meter is 2%. In Tab. 1 the average results for three repetitions are shown for a (mean) target flow rate of 333 nL/min and 2000 nL/min.

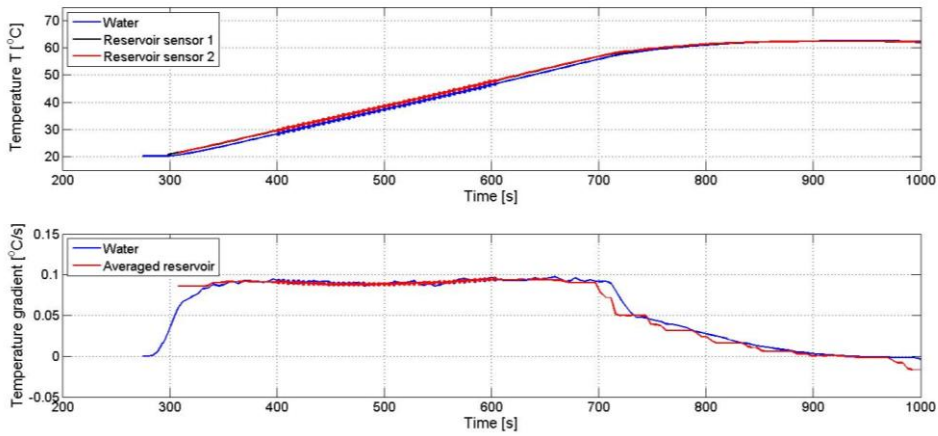


Figure 4 Measured temperature of the expanding liquid (water inside the reservoir) and the reservoir itself. The temperature gradient follows from this temperature and results in the flow rate shown in Fig. 5.

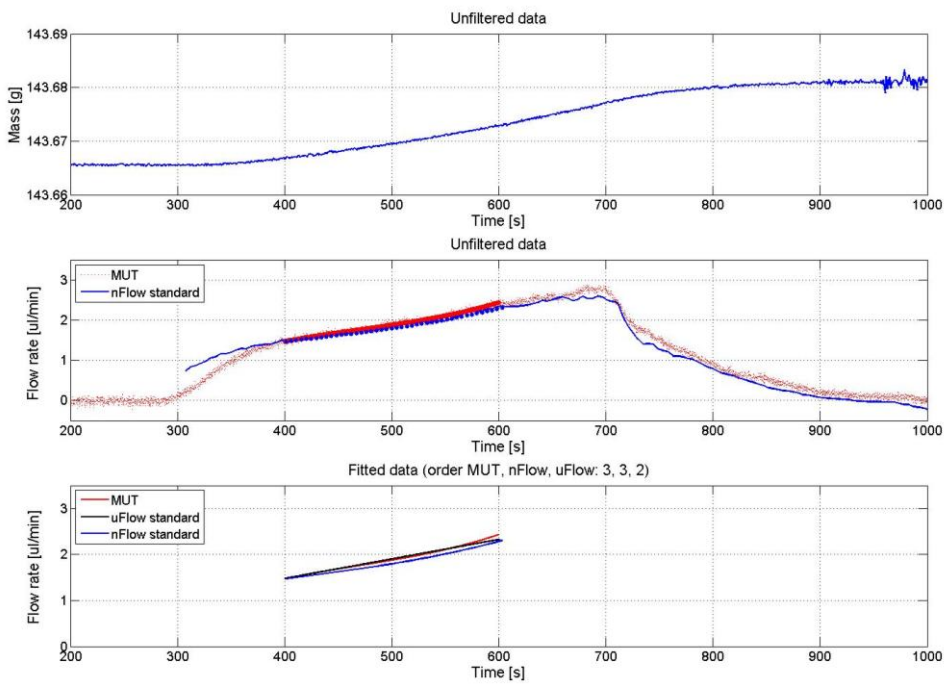


Figure 5 Results comparison volume-expansion standard, a gravimetric standard and the chip-based Coriolis flow meter. The upper graph is the balance read out, the middle part the flow rate according to the chip-based flow meter and volume-expansion standard. The lower graph is the filtered flow rate of the three measurement standards which followed from linear regression of the 'unfiltered data'. The part between 400 s and 600 s is used to determine the average flow rate because in this part the temperature gradient is constant in the reservoir.

*Table 1 Results comparison volume-expansion standard (vol. exp.), a gravimetric standard (grav.) and the chip-based Coriolis flow meter (cori). For two target flow rates (333 nL/min and 2000 nL/min) three repetitions have been performed. The mean flow rate is given by  $\hat{Q}$  and the relative standard deviation by  $\sigma$ .*

	target: 333 nL/min		target: 2000 nL/min	
	$\hat{Q}$ (nL/min)	$\sigma$ (%)	$\hat{Q}$ (nL/min)	$\sigma$ (%)
vol. exp	364	2.1	1776	2.8
grav.	372	2.4	1816	2.5
cori	375	1.5	1796	3.3

sensor. *Journal of Micromechanics and Microengineering*, 20(6). p. 125001. ISSN 0960-1317

## REFERENCES

[1] Ahrens, M., Klein, S., Nestler, B. and Damiani, C., Design and uncertainty assessment of a setup for calibration of microfluidic devices down to 5 nL min<sup>-1</sup>, *Measurement Science and Technology*, volume 25, 2014

[2] Cox, M.G., Harris, P.M., Software support for metrology best practice guide no. 6 – uncertainty evaluation, *NPL technical report*, 2006.

[3] Gersl, J. Numerical results for nano-flow generator fo VSL, technical report available at [http://www.drugmetrology.com/images/Gersl\\_Numerical\\_Simulations\\_NFG.pdf](http://www.drugmetrology.com/images/Gersl_Numerical_Simulations_NFG.pdf)

[4] Lucas, P. *et al.*, *Metrology for drug delivery*, 2012 - 2015, partners VSL, Cetiat, CMI, DTI, EJPD, IPQ, Tubitak, project summary at [http://www.euramet.org/index.php?id=emrp\\_call\\_2011](http://www.euramet.org/index.php?id=emrp_call_2011)

[5] Tanaka, M. *et al.*, Recommended table for the density of water between 0 °C and 40 °C based on recent experimental reports, *Metrologia*, 38, 301-309, 2001

[6] Sparreboom, W., Geest, J. van de, Katerberg, M., Postma, F., Haneveld, J., Groenesteijn, J., Lammerink, T. Wiegerink, R. J. and Lötters, J.C. (2013) Compact mass flow meter based on a micro coriolis flow sensor. *Micromachines*, 4(1). pp. 22-33. ISSN 2072-666X

[7] Haneveld, J., Lammerink, T.S.J., Boer, M.J. de, Sanders, R.G.P., Mehendale, A. and Lötters, J., Dijkstra, M.A., and Wiegerink, R.J. (2010) Modeling, design, fabrication and characterization of a micro Coriolis mass flow